Benchmarking of UAV Guidance Systems in Nap of the Earth (NOE) Flight

Eric N. Johnson
eric.johnson@aerospace.gatech.edu
Lockheed Martin Associate Professor of Avionics Integration

Dmitry Bershadsky
dbershadsky@gatech.edu
Graduate Student

Georgia Institute of Technology
Atlanta, GA, USA

ABSTRACT

This paper describes the development of a proposed framework of metrics for the evaluation of the performance of aircraft guidance systems. The methodologies and metrics developed remain generally agnostic to whether or not the aircraft is manned. Although more complicated missions such as autonomous exploration/search, ferry, surveillance, multi-agent collaboration, and manned flight may be addressed at a later time, A-B flight scenarios are chosen to study the proposed metrics. The proposed metrics will form building blocks for the more complicated missions. Metrics development has thus far generally focused on NOE flight, and in particular on the observability of the vehicle throughout its mission. That is, a formulation of probability of detection by potential and generally unknown threats in the mission area will be the main metric. Secondary metrics provide insight into the vehicle's trajectory quality in terms of safety and comfort, experienced by both humans and machines are described as well. Scalability of the benchmarking system is also important and benchmarking should be general enough to allow guidance algorithms to be graded independently of the vehicle platform, for instance. Non-dimensionalization metrics will address this concern.

INTRODUCTION

There exists much research into the development of guidance systems for a multitude of types and sizes of vehicles. Many of the relevant works provide benchmarking results or other performance data relating to their respective systems in certain situations or environments (Ref. 1-11). Works relating to ground vehicle, mars exploration, and other robotics tasks have been well studied [ref]. There has not been however any extensive work to provide any sort of relativistic benchmarking between these systems; that is, to provide insight into the evaluation of the performance of these algorithms and systems relative to each other. One such benchmarking framework (Ref. 12) establishes a set of virtual geometric primitives through which systems may be exercised. While this approach is applicable to a specific class of vehicles executing a particular mission, it is not applicable to more general missions or vehicles. For example, consider table 1 which describes a set of autonomously guided rotary winged flights and the corresponding reported top speeds reached.

Table 1: Maximum reported flight speeds achieved (Ref. 13-17)

Organization	speed (ft/s)
UTRC (2012)	7
UCSC (2008)	13
CMU (2008)	33
GT (2012)	50

Suppose that one is interested in comparing the performance of these aerial systems. Based on these data, it may be tempting at first glance to conclude that the 2012 AFDD flight had the "best" results, as the speed attained during the flight is the highest. However, these are difficult to compare for several reasons. What was the mission? What about vehicle characteristics? What sort of vehicle was it and of what scale? What equipment was used, and what sensors were employed? Was the guidance system relying on GPS, vision, laser rangefinder, or another navigation aide? What about the environment through which the vehicle traversed? Was the vehicle tasked with navigating a passive obstacle field, with wires, and buildings? Was it a flight test or a simulator result? Were there active threats? What about considerations of safety in terms of exposure, vulnerability, or closest approach to obstacles? There is no clear method of comparing the performance of these systems. In relation to the above, how is it possible to, in a meaningful way,

compare the guidance system of the AFDD's relatively high-altitude flight with a JUH-60 to that of UTRC's flight with a vehicle three orders of magnitude lighter? It is clear that, without scoping the problem, the considerations will quickly increase the difficulty of the problem. As mentioned, this paper attempts to scope the problem by focusing on NOE flight, and presents metrics of primary and secondary importance that allow direct comparisons of guidance algorithms and systems to each other in such a mission. The paper describes the development of these and discusses simulation results and those of a flight test.

METRIC DEVELOPMENT

A set of primary and secondary metrics are proposed for development. Metric components investigated consider vehicle states, capabilities, and characteristics of the environment. The primary metrics focus on the observability or the probability of detection by a threat in the vehicle's environment. Secondary metrics focus on energy efficiency, constraint violations, and the like and are briefly discussed.

Primary metrics developed

The first primary proposed metric for NOE flight scenarios is termed the visibility metric (VM). This scalar value generated based on the area of the reverse viewshed, or the time integral of the area from which the vehicle is visible integrated over the time period of interest. The viewshed area is non-dimensionalized by the projected area traversed by the vehicle, or the disc/wing area, depending on the application. One application of this metric is described below in the simulation section. The metric provides the basis of an observability comparison between different aircraft operating around the same area, or the same aircraft operation with different conditions. The example given is that of a helicopter flying NOE trajectories over a small town at differing speeds and altitudes. The metric is applied to provide insight as to how the UAS performs in terms of visibility under differing conditions. Associated with this metric is the mean VM over the flight. This gives an indication as to the average exposure of the vehicle throughout its flight, removing the time aspect included in VM. This is discussed below.

The second primary metric is the height above terrain is integrated over the time of the flight. A lower value of this metric is "better" in terms of safety and detectability, which is implicitly the basis of NOE tactics. This metric is scaled by the longest dimension of the vehicle to allow a more fair comparison between vehicles. Both metrics give an indication as to the observability of the vehicle in terms of one or more uniformly distributed observers in the environment.

Proposed secondary metrics

Secondary metrics proposed provide insight into other aspects of overall vehicle safety and mission performance. These are relative to both external and self constraints. Vehicle rates calculated over the flight, and in particular, velocities and accelerations are compared to internal constraints. These may be imposed by vehicle or payload capabilities for example. When non-dimensionalized by the maximum allowable respective limits, these metrics provide a partial figure for safety and maneuvering aggressiveness in terms of remaining control authority and vehicle capability margins throughout the flight. The closest approach to obstacles may also calculated when feasible and also contributes to the overall safety metric. Waypoint precision/route deviation may also be considered when feasible and applicable. An energy use metric may also be added as another secondary output. These are further described in the future work section.

SIMULATION AND FLIGHT TEST

Two simulation systems are used to investigate the primary metrics described by this paper. Together, the tools form a system to investigate the benchmarking of UAV guidance algorithms, although the metrics are general enough to be investigated by any tools capable of calculating a viewshed of a vehicle navigating in an environment. The first tool, NOE Simulation Tool (NOEST), is developed for this study and used to examine missions at a high level and large range scale. This simple tool provides a simple trajectory generator for a point mass vehicle and allows the user to calculate the viewshed of the vehicle in a terrain environment. High-level visibility metrics for A-B flights over multiple miles over varying terrain may be calculated using a simple vehicle model.

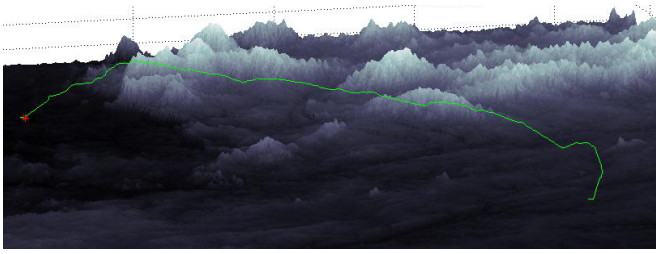

Figure 1. NOEST with a digital terrain elevation database and recorded Cessna 172 flight path

The level of the metrics depends on the level of detail of the terrain model. Figure 1 shows a digital terrain elevation database (DTED) representation of northern Georgia with a vehicle trajectory, described below. The second tool, the Georgia Tech UAV Simulation Tool (GUST), is a high fidelity full UAS simulator and is used is used to test metrics

to a higher level of fidelity and with more degrees of freedom than with the NOEST. In addition to primary metrics, secondary metrics may now be investigated with finer attention to detail by populating scenarios with buildings, poles, and other objects.

In order to calculate VM in simulation, we have chosen to generate a grid of potential observers in the area of vehicle operation. Computationally, the area of operation of the vehicle is discretized to form a regular grid of pixels. This is shown in figure 2.

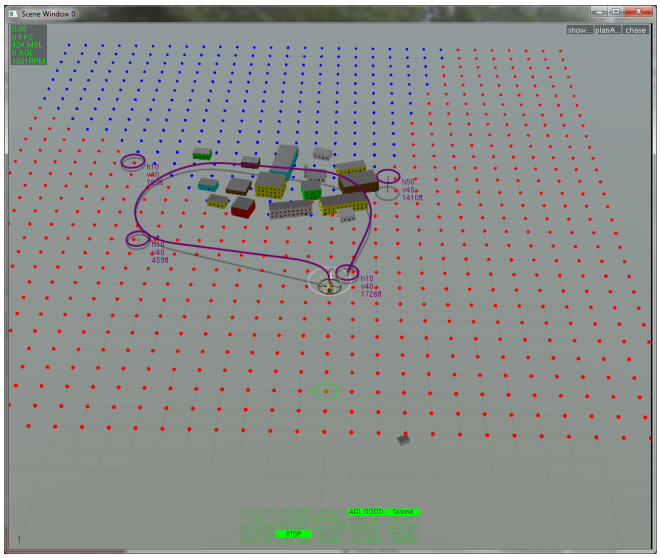

Figure 2. GUST showing instantaneous viewshed around simulated buildings

In the figure, red pixels denote grid points that can see the vehicle (or vise versa), and blue grid points are obscured. Line of sight visibility is calculated to every pixel at every time step to generate these data. A maximum range is also used for this formulation in an effort to account for atmospheric, geometric, and other environmental effects. This could be modified in the future to account for aspects such as: the curvature of the earth, types of observers, more complex atmospheric models, and geometric effects based on vehicle attitude and size.

NOEST

NOEST utilizes digital terrain elevation data (DTED) from the Shuttle Radar Topography Mission (SRTM) over a specified range of latitude and longitude to form an arena. The tool includes a simple trajectory generator for a point mass helicopter that is described below. The tool also allows a state trajectory to be imported from a separate vehicle simulator or other source. Threats with various characteristics (types, positions, altitudes, detection and engagement ranges, etc) may be added in specified locations or uniformly distributed inside the flight area. The state trajectories are then graded based on the metrics described in this document. The tool outputs several metrics calculated using the flight's trajectory and terrain information.

The simple trajectory generation is based on a 6DOF point-mass aircraft model. The model includes position and velocity states and takes accelerations as inputs for the time being. The vehicle attempts to reach a destination and use the gradient information in the vicinity to attempt NOE-like flight. To perform any real optimization is out of scope for this project as the tool allows importing trajectories generated by other tools or flight tests.

Threats are currently modeled as static, point objects residing on the surface of the terrain in specified or uniformly distributed locations. Mobile and air threats may also be added in the future. In reality, threats are not uniformly distributed. Game theory should be investigated to better understand the placement of threats in the environment.

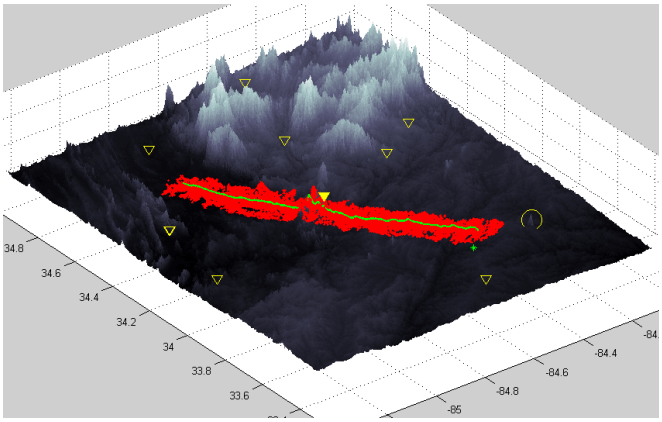

Figure 3. DTED map between PDK and DNN airports. Axes in degrees latitude and longitude.

Figure 3 shows a sample NOE flight from PDK to DNN airports near Atlanta. The red region is the reverse viewshed composite calculated over the green flight trajectory. A simple line of sight model is implemented (to be described). The terrain height is exaggerated bout 300%. Triangles denote threats and solid triangles are threats that have detected the vehicle based on the line of sight model described. Some landmarks are included as well; the green asterisk is Georgia Institute of Technology and the yellow circle is Stone Mountain. The area is formed by 1200x600 approximately 1/2 mile pixels. The distance between the airports is around 40 miles. No buildings or trees or any other data are added. A plot of arbitrary pixel index and the overall time for which they can see the aircraft is shown below in figure 4a. The same data are shown for an actual flight in a Cessna 172 in figure 4b. Both are sorted in order of total visibility time per respective pixel.

As expected, the amount of pixels with line of sight to the aircraft are higher for a longer amount of time in the Cessna flight as compared to that of the NOE flight.

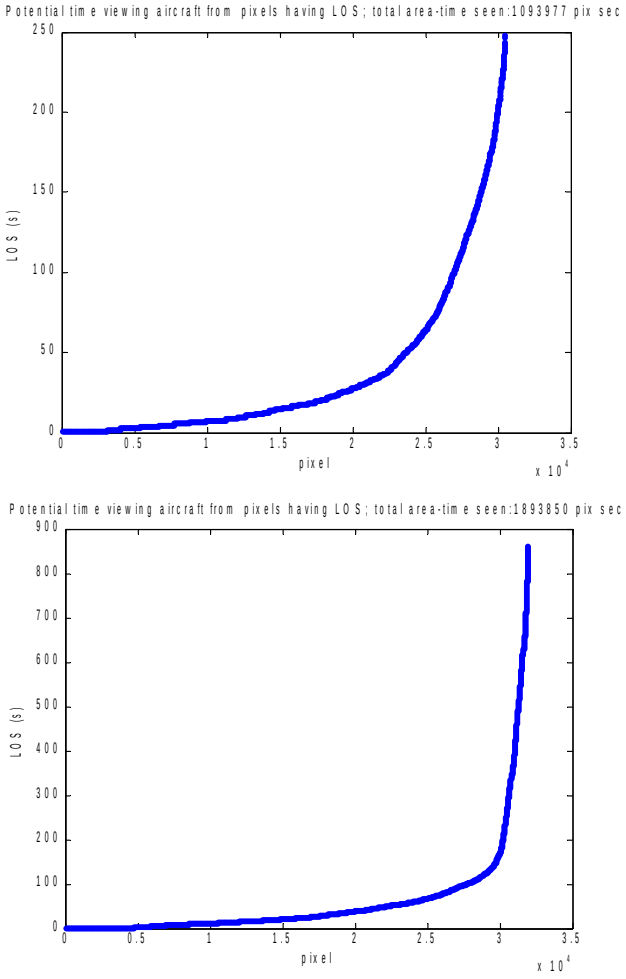

Figure 4. (a. top) NOE simulated flight at 50 ft, (b. bottom) Cessna 172 flight at 5,000 ft nominal.

GUST

An example flight of a Yamaha RMAX helicopter is shown in figure 5 following an NOE trajectory. This is flown at the McKenna MOUT site at Fort Benning. The grid size used is 15 ft between each point. The helicopter is visible near the bottom middle of the figure flying clockwise along the oval purple path, between the second and third buildings along its path.

Figure 6 shows a primary metric, VM, for this flight scenario. In this case, VM is scaled by the entire grid area in the flight environment. Nine total scenarios are simulated, each with a different nominal flight altitude and at a different commanded flight speed. Three runs at clearance altitudes of 20, 40, and 70 ft are run at 30, 50, and 70 ft/s commanded flight speed. Obstacles are detected by a simulated forward facing lidar scanner (a SICK LD-MRS) with a range of about 100 ft. The characteristic first dip in VM is seen in the 20 and 40 ft flights.

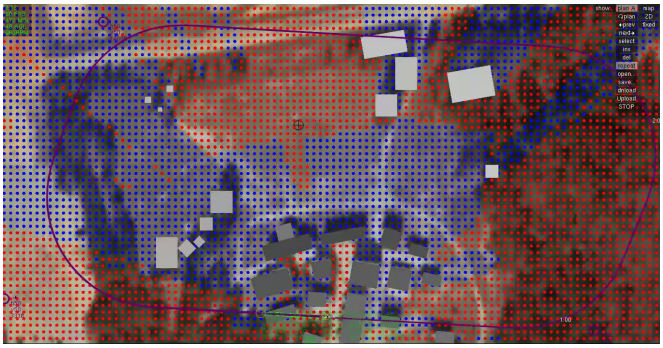

Figure 5. Georgia Tech UAV Simulation Tool (GUST) showing viewshed grid calculated at an instant in time during a flight. Blue dots indicate masked regions, red dots indicate areas from which the vehicle is not masked.

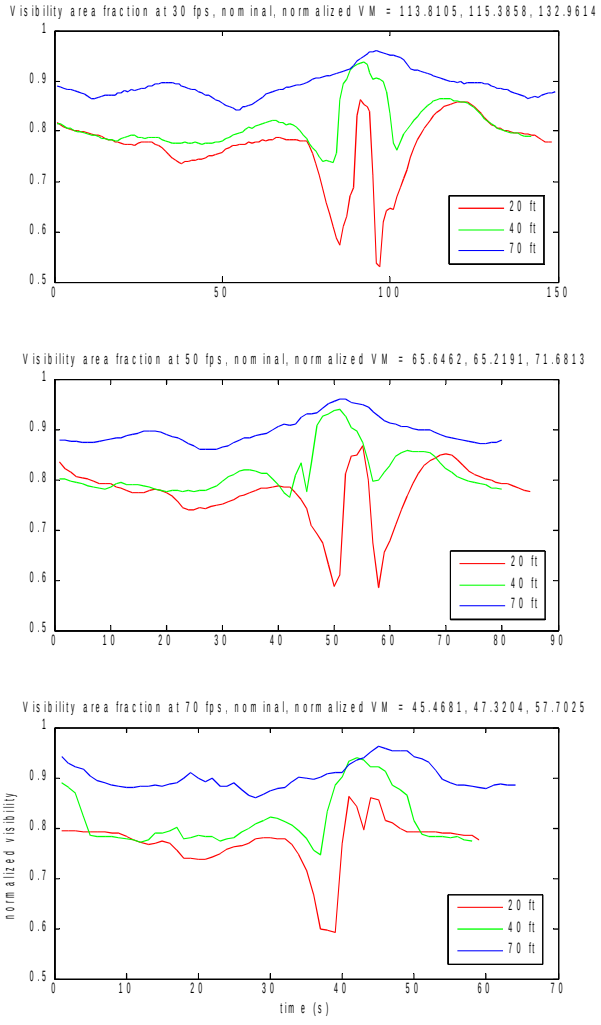

Figure 6. VM over the nine NOE flight scenarios

This occurs when the vehicle is masked by the first building in its path. As the vehicle climbs over the building, VM increases until the vehicle drops behind it and is masked again.

The vehicle then climbs over the third building and continues its flight. Notice that at 70 ft/s, the vehicle does not have space or time to dip behind the second building unlike the slower flights. VM suffers as a result instantaneously, but because the overall flight is quicker, the total VM is lower.

Table 2 shows the data from the flight. The top half of the table shows VM integrated throughout the flight. The bottom half shows the VM integration normalized (VM n) with the time of each circuit. In other words, this is the average VM per flight. Note that VM for the 20 and 40 ft cases are statistically similar. This is due to the fact that while the 20 ft case has a lower average VM, the flight took more time due to more intense climbs and descents. This provides a sanity check for the algorithm, as the speed of the aircraft should not change the average VM at an instantaneous point during the flight. Note that VM n is then mainly a function of altitude.

Table 2. VM and mean VM for the nine NOE flight scenarios

VM	30 fps	50 fps	70 fps
20 ft	113.8	65.6	45.5
40 ft	115.4	65.2	47.3
70 ft	133	71.7	57.7

VM n	30 fps	50 fps	70 fps
20 ft	0.76	0.77	0.76
40 ft	0.82	0.85	0.84
70 ft	0.92	0.90	0.92

CONCLUSIONS

All primary metrics tend to be a function of the vehicle's states, primarily of position and attitude. For NOE A-B flight scenarios, instantaneous exposure is not a function of speed for otherwise similar cases. If instantaneous exposure is desired, the time average of VM should also be considered. That is, the VM metric may be deceiving if the vehicle is moving very quickly – VM is lower because the overall time is less as compared to the case with a slower UAS, but the mean or instantaneous VM should also be considered. It may be safer for instance to fly slower but trace a different path between buildings and trees. Of course, this is also situational, and this point should be kept in mind.

Observability or exposure is not linear with respect to altitude. That is, halving altitude doesn't necessarily halve the vehicle's observability, but of course, this is a general conclusion and is situational.

As this work focuses on standard aircraft in NOE flight, an acoustic version of VM should be addressed. A simple acoustic propagation model will be implemented to augment the observability metric. This model is yet to be selected but will give a more complete metric of exposure of a vehicle in NOE flight. In addition, it is recommended that secondary metrics be investigated more thoroughly. This will allow for more careful comparison between UAS in cases where a feasibility metric is required.

REFERENCES

[1]Kondraske, G. and Khoury, G., "Telerobotic System Performance Measurement: Motivation and Methods," in Proceedings of SPIE, Vol. 161, SPIE, 1992.

[2]Skubic, M., Kondraske, G., Wise, J., Khoury, G., Volz, R., and Askew, S., "A Telerobotics Construction Set with Integrated Performance Analysis," In proceedings of the IEEE/RSJ International Conference on Human Robot Interaction and Cooperative Robots," Intelligent Robots and Systems '95. 3, 1995.

[3]Sukhatme, G. and Bekey, G., "Multicriteria Evaluation of a Planetary Rover," in Proceedings of the Planetary Rover Technology and Systems Workshop, IEEE International Conference on Robotics and Automation, pp. 22–28.

[4]Evans, J. and Messina, E., "Performance Metrics for Intelligent Systems," NIST SPECIAL PUBLICATION SP, 2001, pp. 101–104.

[5]Wong, S., Middleton, L., MacDonald, B., and Auckland, N., "Performance Metrics for Robot Coverage Tasks," Proc. 2002 Australasian Conference on Robotics and Automation, Vol. 27, 2002, p. 29.

[6]Tunstel, E., "Operational Performance Metrics for Mars Exploration Rovers: Field Reports," *Journal of Field Robotics,* Vol. 24, No. 8-9, 2007, pp. 651–670.

[7]Schreckenghost, D., Fong, T.W., Milam, T., Pacis, E., Utz, H., "Real-Time Assessment of Robot Performance during Remote Exploration Operations," Aerospace Conference, March, 2009.

[8]Nehmzow, U., Robotics and Autonomous Systems, Vol.44, No. 1, 2003, pp.55–68.

[9]Albus, J., "Metrics and Performance Measures for Intelligent Unmanned Ground Vehicles," NIST Special Publication, 2002, pp.61–68.

[10]Meystel, A., "Performance of Planning Systems," NIST Special Publication, 2002, pp.99–104.

[11]Freed, M., Harris, R., & Shafto, M. (2004). Measuring Autonomous UAV Surveillance Performance. Proceedings of PerMIS, 2004.

[12]Mettler, B., Kong, Z., Goerzen, C., and Whalley, M., "Benchmarking of Obstacle Field Navigation Algorithms for Autonomous Helicopters," presented at the American Helicopter Society 66th Annual Forum, Phoenix, AZ, May 2010.

[13]Whalley, M., Takahashi, M., Tsenkov, P., Schulein, G., Goerzen, C., "Field-Testing of a Helicopter UAV Obstacle Field Navigation and Landing System," Proceedings of the 65th Annual Forum of the American Helicopter Society, 2009.

[14]Sebastian Scherer, Sanjiv Singh, Lyle J. Chamberlain, and Mike Elgersma, "Flying Fast and Low Among Obstacles: Methodology and Experiments," The International Journal of Robotics Research, Vol. 27, No. 5, May, 2008, pp. 549-574.

[15]Sebastian Scherer, Lyle J. Chamberlain, and Sanjiv Singh, "First Results in Autonomous Landing and Obstacle Avoidance by a Full-Scale Helicopter," ICRA, May, 2012.

[16]Tsenkov, P., Howlett, J.K., Whalley, M., Schulein, G., Takahashi, M., Rhinehart, M.H., Mettler, B., "A System for 3D Autonomous Rotorcraft Navigation in Urban Environments," AIAA Guidance, Navigation, and Control Conference, Honolulu, HI, 2008.

[17]Johnson, E. N., Mooney, J. G, Ong, C., Hartman, J., Sahasrabudhe, V., "Flight Testing of Nap-of-the-Earth Unmanned Helicopter Systems", Proceedings of the 67th Annual Forum of the American Helicopter Society, Virginia Beach, VA, 2011.